

Prediction of Wing Downwash Using CFD

Mohammed MAHDI*

*Corresponding author

Aeronautical Research Center-Sudan, P.O. Box 13342

momahadi2007@hotmail.com

DOI: 10.13111/2066-8201.2015.7.2.10

3rd International Workshop on Numerical Modelling in Aerospace Sciences, NMAS 2015, 06-07 May 2015, Bucharest, Romania, (held at INCAS, B-dul Iuliu Maniu 220, sector 6) Section 5 – New concepts in UAV systems

Abstract: Wing downwash study and estimation of downwash effect on the tail plane is an important task during the aircraft design process, although a lot of papers and works has been done, but the experimental work is the most important, the progress in CFD simulation has reached to the point it is able to reduce the number of runs in the wind tunnel. In this work CFD has been utilized to calculate the downwash angle and downwash gradient with respect to the angle of attack over a high aspect ratio of a typical UAV. The results of the simulation shall be used in the estimation and calculation of the longitudinal static stability analysis of the UAV.

Key Words: wing downwash, CFD, static longitudinal Stability, UAV

1. INTRODUCTION

Downwash is the air forced down by the aerodynamic action of wing or helicopter rotor blade in motion, as part of the process of producing lift (Wikipedia, [1]).

Several studies to analyze the behaviour of wing downwash have been made. Jurkovich, 2011 [2] has applied the CFD approach to the prediction of the downwash flowfield behind a KC-135 tanker. The results show the criticality of capturing the trailing vortex behind the wing using a fine mesh out into the far field. The results are compared to the theory, vortex lattice results, and wind tunnel data. While numerical dissipation is evident in the premature spreading of the vortex core, this does not affect the downwash flowfield, which is the critical factor in aerial refueling. Euler solutions with properly applied gridding are shown to be sufficient for capturing the tanker flowfield for aerial refueling needs.

Anad & Kukami, 2014, [3] have studied the aerodynamics performance of wing canard configuration using the CFD analysis and they simulated the flow path lines and particles flow field over the canard-wing configuration to estimate the best vertical positioning of the canard with respect to the wing.

In our work we will study the flow field properties of a typical UAV high aspect ratio wing; the wing dimensions are tabulated in table 1.

Table 1 wing dimensions of typical UAV

Wing Area	12.1	m ²
Wing span	15.2	M
Root chord	1.12	M
Tip chord	0.47	M
Wing airfoil	E 396	

2. NUMERICAL MODELING

The flow field is solved using incompressible Navier Stokes Equation for the wing and whole aircraft analysis.

The mass conservation law and the energy equation are solved with the Navier-Stokes equations; the K-omega SST turbulence model was used to predict the drag accurately.

For analyzing the studied wing, the flow is assumed to be incompressible due to the maximum speed is 50(m/s). So only Navier stokes equations with the K-Omega and continuity equation are solved simultaneously (Chung, 2002, [4]).

Mass conservation law:

$$\frac{\partial u_i}{\partial x_j} = 0 \tag{1}$$

Navier-Stokes Equations: These equations were employed in the following form [20]:

$$\frac{\partial \vec{q}}{\partial t} + \frac{\partial \vec{E}}{\partial x} + \frac{\partial \vec{F}}{\partial y} + \frac{\partial \vec{G}}{\partial z} = \frac{\partial \vec{R}}{\partial x} + \frac{\partial \vec{S}}{\partial y} + \frac{\partial \vec{T}}{\partial z} \tag{2}$$

where

$$\vec{q} = \rho \begin{bmatrix} 1 \\ u \\ v \\ w \end{bmatrix}, \vec{E} = \rho \begin{bmatrix} u \\ u^2 + p/\rho \\ uv \\ uw \end{bmatrix}, \vec{F} = \rho \begin{bmatrix} v \\ uv \\ v^2 + p/\rho \\ vw \end{bmatrix}, \vec{G} = \rho \begin{bmatrix} w \\ uw \\ vw \\ w^2 + p/\rho \end{bmatrix}, \vec{R} = \begin{bmatrix} 0 \\ \tau_{xx} \\ \tau_{xz} \\ \tau_{xz} \end{bmatrix},$$

$$\vec{S} = \begin{bmatrix} 0 \\ \tau_{yx} \\ \tau_{yy} \\ \tau_{yz} \end{bmatrix}, \vec{T} = \begin{bmatrix} 0 \\ \tau_{zx} \\ \tau_{zy} \\ \tau_{zz} \end{bmatrix}$$

Selection of turbulence model depends on the type of grid i.e., structure or unstructured grid. Accordingly for the present simulation K-omega SST turbulent model was used for the purpose of turbulence closure.

This model has wide spread popularity among the CFD researchers. For more information about this model, see Menter, 1994, [5].

He states that this model is more accurate than k-epsilon especially near wall layers, and for flows with moderate adverse pressure gradients. He developed the SST scheme for aerospace applications as follows.

$$\frac{\partial \rho k}{\partial t} + \frac{\partial \rho u_j k}{\partial x_i} = P_k - \beta^* \rho \omega k + \frac{\partial}{\partial x_j} \left((\mu + \sigma_{k1} \mu_t) \frac{\partial k}{\partial x_j} \right) \tag{3}$$

$$\frac{\partial \rho \omega}{\partial t} + \frac{\partial \rho u_j \omega}{\partial x_i} = \gamma_1 P_\omega - \beta_1 \rho \omega^2 + \frac{\partial}{\partial x_j} \left((\mu + \sigma_{\omega 1} \mu_t) \frac{\partial \omega}{\partial x_j} \right) \tag{4}$$

And since the flow is steady incompressible the above equation becomes simpler. Definition of the eddy-viscosity:

$$v_t = \frac{k}{\omega} \quad (5)$$

Turbulent stress tensor $\tau_{i,j}$ is given by:

$$\tau_{i,j} = v_t \left(\frac{\partial u_i}{\partial x_j} + \frac{\partial u_j}{\partial x_i} \right) - \frac{2}{3} k \delta_{ij} \quad (6)$$

The shear stress is calculated as follows:

$$\tau = \rho a_1 k \quad (7)$$

With the constant $a_1 = 0.3$. On the other hand, in two-equation models, the shear-stress is computed from

$$\tau = \mu_t \Omega \quad (8)$$

The turbulence intensity, I , is defined as the ratio of the root-mean-square of the velocity fluctuations, u' , to the mean flow velocity, u_{avg} .

A turbulence intensity of 1% or less is generally considered low and turbulence intensities higher than 10% are considered high.

The turbulence intensity in the free stream is usually available from the tunnel characteristics.

In modern low-turbulence wind tunnels, the free-stream turbulence intensity may be as low as 0.05%. In this work the turbulence intensity assumed 0.1%.

The turbulent viscosity ratio, μ_t / μ , is directly proportional to the turbulent Reynolds number ($Re_t = k^2 / (\epsilon \nu)$).

Re_t is large (on the order of 100 to 1000) in high-Reynolds-number boundary layers, shear layers, and fully-developed duct flows. However, at the free-stream boundaries of most external flows, μ_t / μ is fairly small. Typically, the turbulence parameters are set so that $1 < \mu_t / \mu < 10$

Boundary Layer Consideration: Boundary layer is calculated based on Reynolds number; the following expression defines the Reynolds No.

$$Re = \frac{\rho_\infty V_\infty \bar{C}}{\mu_\infty} \quad (9)$$

According to Anderson, 2011, [6], the boundary layer thickness is given by:

$$\delta = \frac{0.37x}{Re_x^{1/5}} \quad (10)$$

Grid Generation. Figure (1) shows the surfaces mesh of wing; a fine mesh is focused near a/c surface to smooth surfaces as well as considering the boundary layer effect, the interval size of the element is almost 2.5 (mm), which is created inside ANSYS workbench.

Unstructured grid with triangles and tetrahedral in the surface and volume meshes, approximately 10 million cells, is created in the computational domain of the wing.

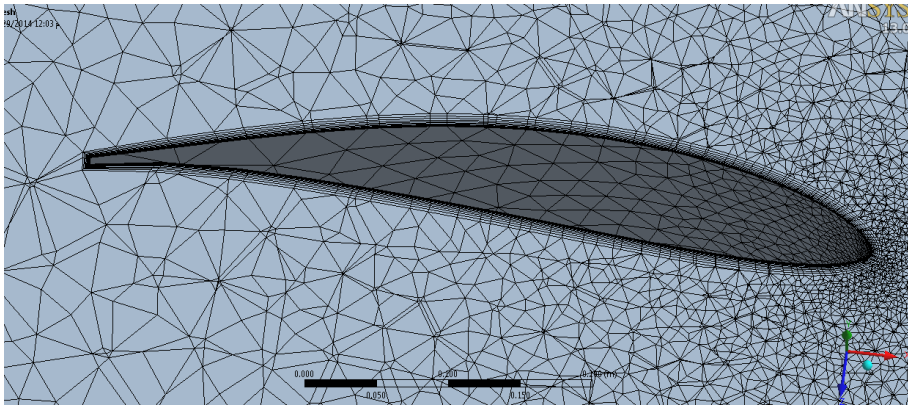


Figure 1 wing mesh and boundary layer is clear

Downwash

Downwash is the air forced down by the aerodynamic action of a wing or helicopter rotor blade in motion, as part of the process of producing lift, an aircraft produces aerodynamic lift by deflecting air downwards as downwash. As shown in figure 2, downwash generates an equal and opposite upwards force on the wing, called lift. When the downwash force exceeds the weight of the aircraft, the aircraft will rise since there is a considerable pressure difference between the lower and upper surfaces of a wing; tip vortices are produced at the wingtips [4].

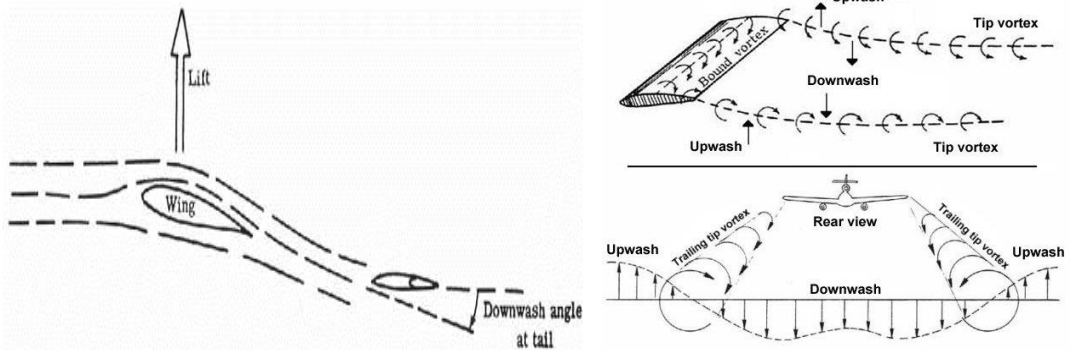


Figure 2 Downwash Definition

The downwash is estimated from the CFD, that rake line is constructed along the aerodynamics axis of the HT, and then the downwash effect on the tail is plotted vs. HT semi span.

According to Biot-Savart law the vortex will induce downwash due to induced velocity and given by

$$\varepsilon = \arctan\left(\frac{w}{V_\infty}\right) \cong \frac{w}{V_\infty} \tag{11}$$

So; the wing downwash could be calculated from the formula:

$$\varepsilon = -\tan^{-1}\left[\frac{-V_z \cos \alpha + V_x \sin \alpha}{|V|}\right] \tag{12}$$

Results

Figure 3 shows the flow path lines colored by velocity magnitude at $\alpha=0$; the flow is attached to the upper surface and no vortex is captured in the upper surface, the wing tip vortices is weak and a little twist observed in the flow at the tip.

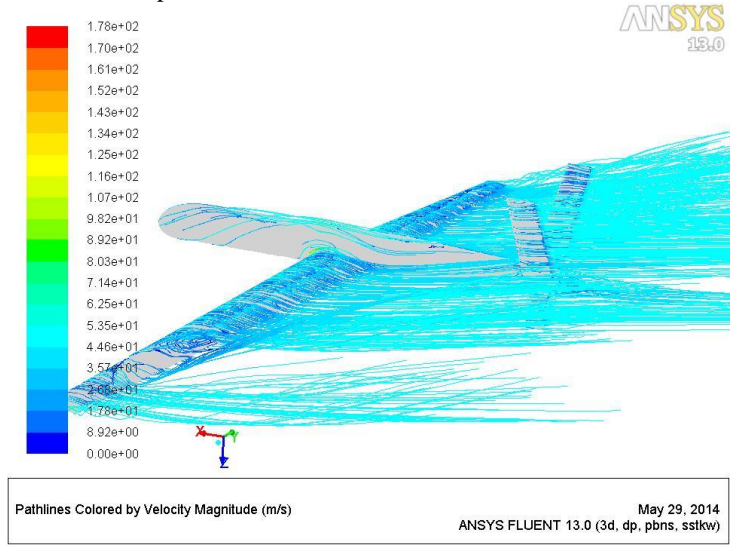


Figure 3 Flow Pathlines colored by velocity magnitude at $\alpha = 0$

Figure 4 shows the flow path lines over the upper surface of the wing at $\alpha = 16$. This figure indicates an existence of vortex on upper surface and tip vortices. The vortices zones are captured by the pencil and zoomed as shown in Figure 4 This figure reveals that, the separation occurs near wing root first and starts to extend span-wisely by increasing the angle of attack. Due to vortices near the wing root trailing edge it is predicted that the wing flap may not be effective at $\alpha > 12 \text{ deg}$.

Wing tip vortices also have high kinetic energy to swirl and rotate which increase the induced drag as a result; these tip vortices will then roll up and get around the local edges of a wing. This phenomenon will reduce the lift at the wingtip station, so they can be represented as a reduction in effective wing span.

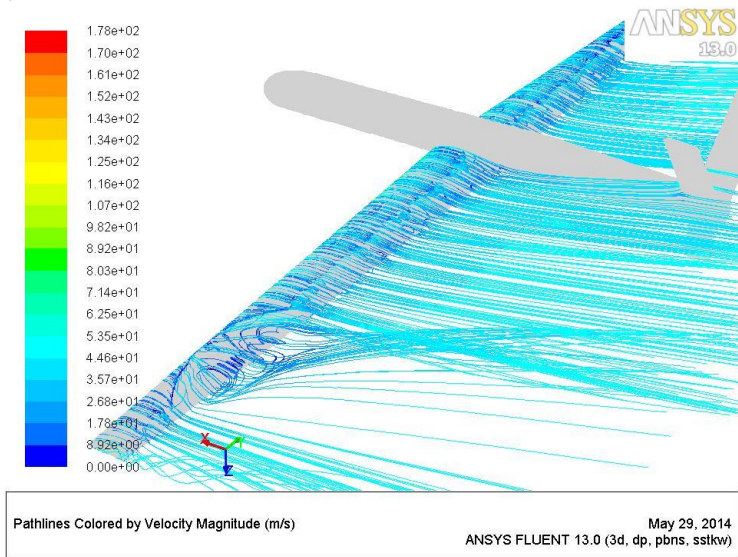


Figure 4 Flow vectors colored by velocity magnitude at $\alpha=12$

Downwash effect on Vee tail at $\alpha=0^\circ$ is shown in Figure 5,

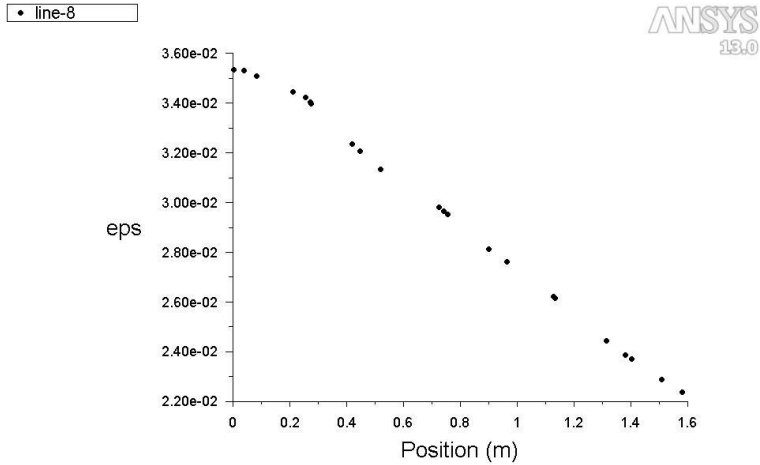


Figure 5 Downwash distribution along Vee tail quarter chord

A line is constructed along the quarter chord line of Vee tail, and the downwash has been plotted along this line as shown in figure 5. From this figure it is shown that at $\alpha = 0$, the downwash is equal 0.036 rad which is equal 2 degree.

So $\epsilon_0 = 2 \text{ deg}$.

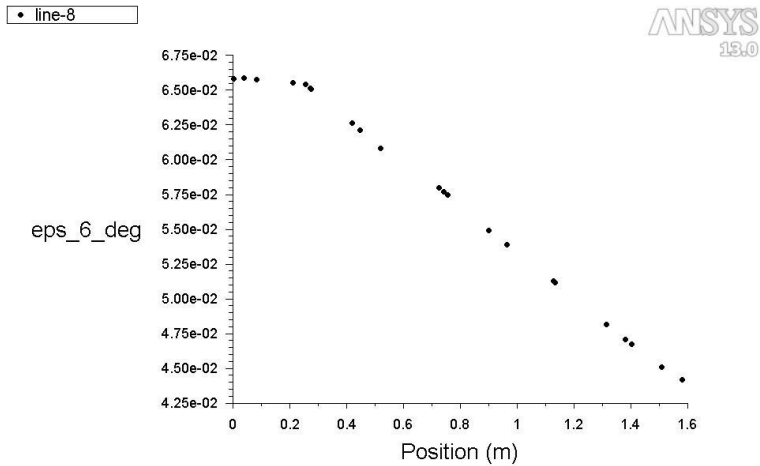


Figure 6 Downwash distribution $\alpha=6^\circ$

From figure 6 So $\epsilon_{\alpha=6 \text{ deg}} = 3.86 \text{ deg}$

$$\text{So } \frac{\partial \epsilon}{\partial \alpha} = \frac{(3.86 - 2)}{(6 - 0)} = 0.31.$$

3. CONCLUSION

From the results obtained the downwash has been calculated efficiently using ANSYS workbench, and this shall be used in the development of the longitudinal stability analysis task during the design process of the UAV.

The CFD shows also the flow pathlines around the vehicles and stall pattern has been figured out.

ACKNOWLEDGEMENT

This work is the properties of ARC; ARC is the funding organization of this work.

REFERENCES

- [1] * * * "Wikipedia", 15 April 2015. [Online]. Available: <http://en.wikipedia.org/wiki/Downwash>.
- [2] M. S. Jurkovich, *CFD Prediction of the Flow field behind the KC-135R Tanker*, 29th AIAA Applied Aerodynamics Conference, 27 - 30 June 2011, Honolulu, Hawaii, AIAA 2011-3510.
- [3] D. R. Anand and P. S. Kukami, *Aerodynamics Performance of Canard-Wing Configuration-A CFD Study*, Bangalore, 2014.
- [4] T. J. Chung, *Computational Fluid Dynamics*, 2nd Edition ed., Cambridge: Cambridge University Press, ISBN 0 521 59416 2 hardback, 2002.
- [5] F. R. Menter, Two-Equation Eddy-Viscosity Turbulence Models for Engineering Applications, *AIAA*, vol. **32**, pp. 1598-1605, 1994.
- [6] J. D. Anderson, *Fundamentals of Aerodynamics*, 5th Edition ed., ISBN-10: 0073398101, New York: McGraw Hill, 2011.